Journal of Marine Research, 41, 747–768, 1983

A subsurface particle maximum layer and enhanced microbial activity in the secondary nitrite maximum of the northeastern tropical Pacific Ocean

by P. C. Garfield,[1] T. T. Packard,[1] G. E. Friederich[1] and L. A. Codispoti[1]

ABSTRACT

Profiles of light transmission, dissolved oxygen, dissolved nutrients, electron transport system (ETS) activity, temperature and salinity were made in the northeastern tropical Pacific Ocean. A particle maximum at 150–300 m within the oxygen minimum and secondary nitrite maximum was associated with the salinity maximum of Subtropical Subsurface Water. A subsurface maximum in ETS activity was also found to be associated with the secondary nitrite maximum and the particle maximum. Persistence of these features at a constant depth and their location within a minimum in vertical static stability suggest an advective and/or *in situ* origin for the particles and an *in situ* development of the associated chemical and biochemical extremes.

1. Introduction

The area of the eastern tropical North Pacific Ocean between 15° and 25° is characterized by several features which make it of interest to oceanographers. Firstly, it is the region of the transition zone between the North Pacific gyral circulation pattern and the equatorial Pacific circulation regime. The boundary between these two regimes is marked by the position of the North Equatorial Current, which, despite seasonal meridional variations in position, is found near the Mexican coast between 15 and 25N (Wyrtki, 1966, 1967; Roden, 1971). Secondly, this area falls within the boundaries of a much larger area where a well-developed oxygen minimum zone is present at intermediate depths. Oxygen concentrations are at or below the lower limits of detection and the presence of a secondary nitrite maximum within these oxygen deficient waters exhibiting nitrite concentrations in excess of 2 μg-at ℓ^{-1} has been documented (Brandhorst, 1959; Thomas, 1966; Goering, 1968; Cline and Richards, 1972; Codispoti, 1973a, 1973b; Codispoti and Richards, 1976).

Subsurface particle maximum layers at intermediate depths in the water column have been reported in two coastal areas where upwelling occurs. Pak and Zaneveld (1978) have reported the occurrence of a particle maximum at intermediate depths off the coast of Oregon which was not associated with an oxygen-depleted layer. Off the

1. Bigelow Laboratory for Ocean Sciences, McKown Point, West Boothbay Harbor, Maine, 04575, U.S.A.

coast of Peru, particle maximum layers at 200 m and 400 m are both within the oxygen minimum layer (Pak *et al.*, 1980; Kullenberg, 1981; Kullenberg and Codispoti, 1982). The shallower particle maximum is also associated with a well-developed nitrite maximum, while the deeper particle maximum is sometimes associated with a weak nitrite maximum. Explanations of these particle layers involve various combinations of the effects of horizontal circulation patterns, elevated surface productivity, offshore transport of the bottom nepheloid layer, dearth of zooplankton due to oxygen depletion and *in situ* bacterial growth. Increased levels of particulate organic material and microbial metabolic rates have been reported to be associated with the 200 m subsurface particle layer off Peru (Garfield *et al.*, 1979; Garfield and Packard, 1979). These facts led us to hypothesize that such particle maximum layers are associated with increased bacterial biomass and/or increased supply of particulate matter available for bacterial metabolism, that they are somehow related to the depletion of oxygen, and that they should be located in other areas where intense oxygen minimum zones are located. We tested these hypotheses during a cruise to the oxygen minimum zone of the eastern tropical North Pacific Ocean aboard the R/V *DeSteiguer*.

This paper reports the presence of another subsurface particle maximum which is associated with the oxygen minimum zone off northwestern Mexico. Vertical and horizontal distributions of nitrite, respiratory electron transport activity and hydrographic variables are presented, and an explanation of the particle maximum is proposed based on these distributions. For purposes of comparison some recent measurements from the N.W. Sargasso Sea and some 1977 data from the Peru Current are also presented.

2. Methods

Samples were collected off the west coast of Mexico (Fig. 1) during January 1981. Temperature, depth, and conductivity profiles were obtained from CTD casts. Samples for analysis of nutrients, oxygen and salinity were taken from a rosette of 5 liter GO-FLO bottles attached to the CTD. Discrete salinity samples analyzed using a Hytech 6220 salinometer were used to calibrate the CTD. Nitrite, nitrate, dissolved silicon, reactive phosphorus and ammonium were determined within 2 h by the methods of Armstrong *et al.* (1967) for nitrite, nitrate and dissolved silicon, Murphy and Riley (1962) for reactive phosphorus, and Slawyk and MacIsaac (1972) for ammonium. All analyses were by the automated procedure described by Friederich and Whitledge (1972). Oxygen concentration determinations were made by Winkler titration. Measurements of light transmission were made by lowering a Hydroproducts (Model 9125) transmissometer to a depth of 300 m at each station. Although the transmissometer was zeroed on deck prior to each cast, maximum percent transmission was sometimes higher than 100%. Therefore, data from each individual profile was normalized to a maximum value of 100% for that station. Each profile represents relative transmission at a given station and can be used to identify maxima

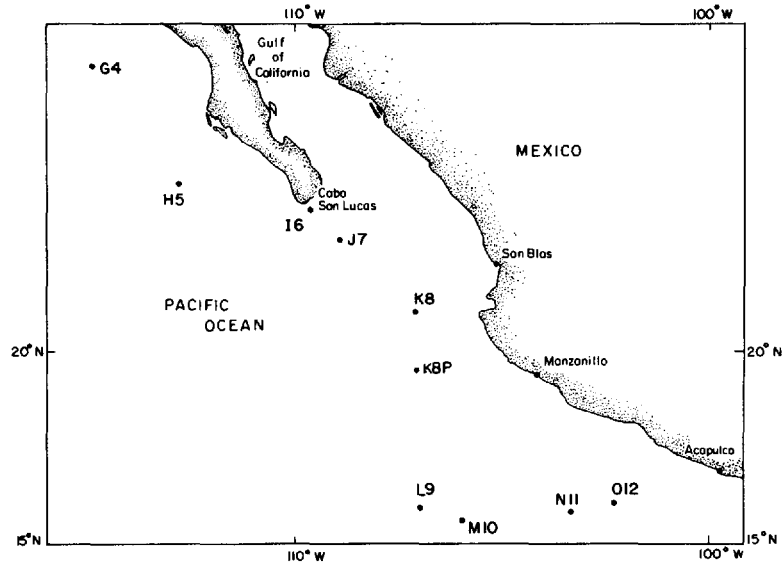

Figure 1. Map of study area for Varifront II cruise aboard the R/V *DeSteiguer*, January 1981.

and minima at that location. However, values of percent transmission are not comparable between stations and the data cannot be plotted as a vertical cross section.

Two separate 30 ℓ Niskin bottle casts at each station provided samples for measurement of ETS activity, nutrients, oxygen, and salinity. Temperature and depth were obtained using reversing thermometers on each bottle. The Niskin bottles were rinsed daily with isopropanol to prevent growth of bacteria. Measurements of respiratory electron transport activity were made using a modification of the tetrazolium reduction technique (Packard, 1969, 1971; Packard *et al.*, 1971; Kenner and Ahmed, 1975). Seawater samples of 20–30 ℓ were filtered through 47 mm Whatman GF/F glass fiber filters at $<1/3$ atm. During the filtration period ($\sim$1 h), the plankton-coated filters were maintained at 0–4°C by immersing the entire stainless steel in-line filter assembly in an ice bath. Seawater samples were never stored longer than 1½ h at 0–4°C before being filtered. Plankton-coated filters were homogenized and activity in the supernatant fluid of centrifuged homogenates was determined by the procedure described by Packard and Williams (1981).

ETS activities are a measure of the maximum potential rate of respiratory electron transport, therefore, we will report ETS activities in units of nanoequivalents (neq) per liter per hour. However, since improvements in ETS methodology during the last ten years (including use of GF/F filters) have resulted in approximately a ten-fold increase in the sensitivity of the method, data from this study expressed as neq are not comparable to previous ETS data without some interpretation. Therefore, these data

have been converted to respiration rates in units of oxygen consumption and denitrification based on respiration:ETS ratios measured in scenescent cultures of aerobic and denitrifying marine bacteria. The ratio is 0.43:1 for oxygen consumption:ETS activity (Christensen *et al.*, 1980) and 1:1.81 for denitrification:ETS activity (Devol, 1975). Since both of these ratios were determined using the old assay method (no Triton X-100), we used a method correction factor of 1:5.0 (old assay:new assay) determined for natural samples of bacteria (Christensen and Packard, 1979) and cultures of marine denitrifiers (Christensen *et al.*, 1980). All three of the above ratios are dimensionless. Our calculated *in situ* rate of oxygen consumption becomes:

$$R_{O_2}\ (\mu\ell O_2\ \ell^{-1}h^{-1}) = \text{ETS}\ (\mu\text{eq}\ \ell^{-1}h^{-1}) \times 0.43 \div 5.0 \times 22.4\,\frac{\mu\ell}{\mu\text{M}} \div 4\,\frac{\mu\text{eq}}{\mu\text{MO}_2}$$

$$\text{or } R_{O_2}\ (\mu\ell O_2\ \ell^{-1}h^{-1}) = \text{ETS}\ (\mu\text{eq}\ \ell^{-1}h^{-1}) \times 0.48$$

and our calculated *in situ* rate of denitrification then becomes:

$$\text{gN m}^{-3}\,\text{y}^{-1} = \text{ETS}\ (\mu\text{eq}\ \ell^{-1}\,\text{h}^{-1}) \div 1.81 \div 5.0 \times 122.7 \div 5\,\frac{\mu\text{eq}}{\mu\text{MN}}$$

$$\text{or gN m}^{-3}\,\text{y}^{-1} = \text{ETS}\ (\mu\text{eq}\ \ell^{-1}\,\text{h}^{-1}) \times 2.7$$

where 122.7 converts units of μMN ℓ^{-1} h^{-1} to gN m^{-3} y^{-1}.

The actual type of respiration occurring in these waters is most likely a combination of oxygen consumption, nitrate reduction and denitrification, however there is currently no means by which the relative rates of these processes can be assessed. Conversion of these data to units of oxygen and nitrogen respiration is based on a number of assumptions which may or may not be true for these waters, however, they are our best estimates of rates of these processes and are valid for comparison with respiratory rates from other areas and using other methods.

Estimates of precision were made by closely spacing three 30 ℓ Niskin bottles on the wire and sampling at a depth of 500 m. Each sample was filtered and analyzed separately, and one sample was stored at 0–4°C for 1½ h prior to filtration. At an ETS activity level of 27 neq ℓ^{-1} h^{-1}, the standard deviation was ± 8% (n = 3).

The Brunt-Väisälä frequency (N) is an estimate of the static stability of the water column, such that stability is high when N is high. Data from the CTD at intervals of 1–2 m were used to calculate N^2, and this resulted in some scatter and some negative values for stability. Negative values signify that the water column is unstable and these were probably the result of the slow response time of the CTD over the depth interval used in the calculations. Therefore, -1.0 was set as the lower limit for N^2 values. Positive values were smoothed somewhat by connecting maximum values to form an envelope enclosing all data points.

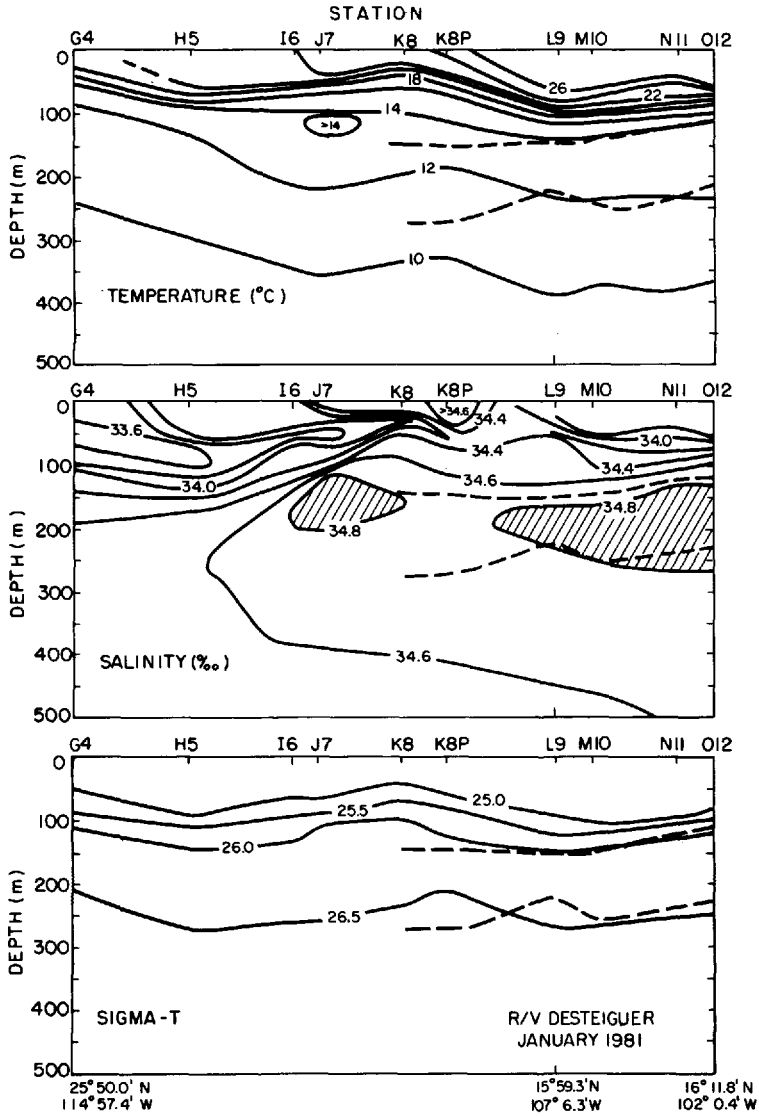

Figure 2. Vertical sections of temperature, salinity, and sigma-*t* along the cruise track shown in Figure 1. Broken lines indicate boundaries of the subsurface particle maximum layer at each station.

3. Results

a. Distribution of water masses. Four water masses of the N.E. tropical Pacific can be readily identified in our temperature and salinity sections (Figs. 2 and 3), all of which have been previously described by Wyrtki (1966; 1967). During this study, California Current Surface Water (CCSW), with salinities lower than 34‰ and temperatures

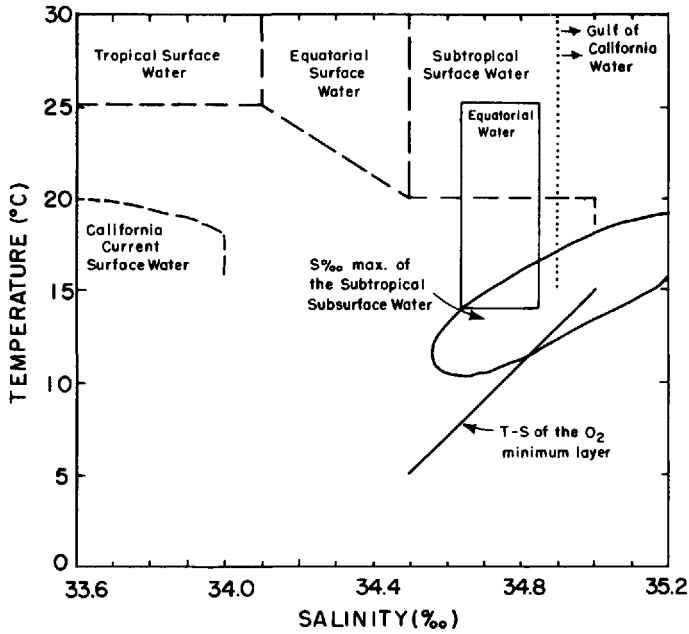

Figure 3. Temperature-salinity diagram of the major water masses in the northeast tropical Pacific Ocean. Gulf of California Water and Equatorial Water are plotted as described by Roden and Groves (1959) and Griffiths (1965). Subtropical Surface Water has been plotted as described for the North Pacific Ocean (Wyrtki, 1967). The remainder of the figure was redrawn from Wyrtki (1967).

lower than 20°C was observed at the surface only as far south as 25N, but it was visible as a subsurface water mass at 50 m to about 20N (K8). Tropical Surface Water (TSW) was present at the surface at the southernmost stations (L9-O12). This was the warmest water encountered, but it was of relatively low salinity due to freshwater runoff. The surface water encountered between 23N and 17N is formed by heating and evaporation of CCSW. When salinities become greater than 34.5‰, this water has been called Subtropical Surface Water by Wyrtki (1967) and Eastern Tropical Pacific or Equatorial Water by Roden and Groves (1959) and Griffiths (1965). The surface salinity maximum found at K8P shows the influence of the warm, salty (>35‰) outflow of the Gulf of California (Griffiths, 1968).

The fourth water mass that we observed in this region forms the well-defined subsurface salinity maximum visible in the section south of Station H5 (Fig. 2). This is Subtropical Subsurface Water (SSW) which has a salinity range of from 34.6‰ to greater than 34.8‰ in this region and a temperature range of 11–14°C (Fig. 3). The northern extent of the SSW is controlled by the influx of California Current Water, which has lower salinity, lower temperature and higher oxygen content.

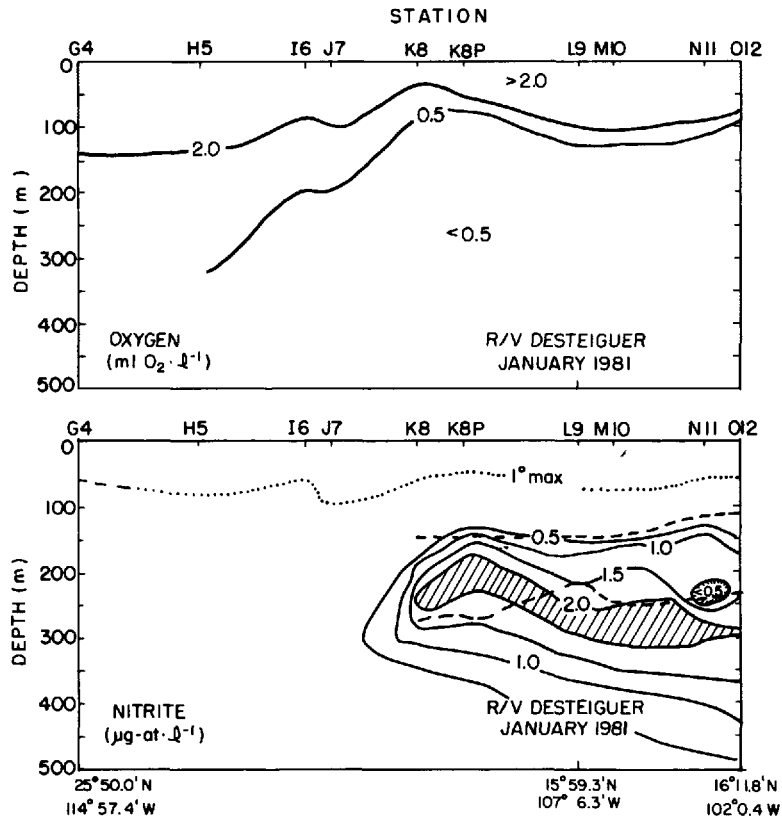

Figure 4. Vertical sections of oxygen concentration (ml O_2 ℓ^{-1}), and nitrite concentration (μg-at $NO_2^- - N$ ℓ^{-1}) along the cruise track shown in Figure 1. Broken lines indicate boundaries of the subsurface particle maximum layer at each station.

b. Distribution of oxygen and nitrite concentrations. The cross section of oxygen concentration (Fig. 4) shows the presence of an oxygen minimum with concentrations of less than 0.5 ml ℓ^{-1} at depths below 75–100 m in the southern half of the section and below 300 m over the whole section. Wyrtki (1967) has shown that the maximum thickness of the oxygen minimum layer where oxygen concentrations fall below 0.25 ml ℓ^{-1} is in excess of 1200 m in this region. The lower portion of this oxygen minimum zone contains a salinity minimum at depths between 600 and 800 m. The water between the salinity minimum and maximum represents a mixtue of these two water types, as indicated by the nearly linear T–S relationship at these depths (Fig. 3 and Wyrtki, 1967).

A distinct secondary nitrite maximum (defined as nitrite concentrations of $\geq$0.5 μg-at ℓ^{-1} below 100 m depth) was present south of 20N (K8) with a thickness of 200–350 m (Fig. 4) and maximum concentrations of ~2.40 μg-at ℓ^{-1}. The intensity of

the maximum appeared to be somewhat decreased east of 105W (N11 and O12), to the extent that at Station N11 there were patches of low nitrite water (<0.20 μg-at ℓ^{-1}) within the maximum. In profile view (Fig. 6) this appears as four separate nitrite maximum layers, the uppermost of which is the primary maximum associated with the euphotic zone.

c. Particle maxima. Light transmission profiles were taken at all ten stations. (We have assumed that a minimum in % transmission is equivalent to a particle maximum, which term will be used in further discussion.) Particle maxima were present in the surface mixed layer at all stations and were probably associated with primary productivity. Distinct subsurface particle maxima were observed near 200 m depth only in % transmission (%T) profiles from the six stations south of 20N (K8-O12) (Figs. 5 and 6). Due to the standardization problem discussed in the Methods section, the data cannot be combined to form a cross section. However, the boundaries of the particle maximum can be defined at each station by a sharp change of 1–2% in the %T signal. (Variability above and below boundaries is ~0.1%.) These upper and lower limits are indicated by the broken lines on the sections of other parameters (Figs. 2 and 4). The top of the 200 m particle maximum layer corresponds closely to the top of the subsurface salinity maximum, the top of the secondary nitrite maximum, the top of the oxygen minimum, and to the depth of the 14°C isotherm. The bottom of the particle maximum layer corresponds to the bottom of the salinity maximum and the core of the secondary nitrite maximum.

The T–S properties of the water between 100 m and 500 m at stations H5 through O12 are shown in Figure 7. Each profile is plotted using a different symbol, and data taken within the particle maximum at every station are represented by an "X". The salinity axis has been offset 0.2‰ for each successive profile. It can be seen that the T–S properties of the water within the particle maximum fall within the subsurface salinity maximum which represents the SSW described above.

Further evidence that the 200 m particle maximum was associated with a water mass and not with a pycnocline is shown in Figure 8 for station K8. The particle maximum and secondary nitrite maximum are located within a zone of minimum static stability, as indicated by low values of N^2. If they were associated with a pycnocline we would find them within a zone of high static stability (e.g., $N^2 > 100$ cph^2). This type of association with a stability minimum is also found for the 200 m particle maximum and nitrite maximum at the other stations. The zone of high stability found above the stability minimum represents the upper boundary of the SSW (depth = 100–150 m). Barber and Huyer (1979) reported a similar situation off Peru, where the secondary nitrite maximum is located in a zone of minimum vertical stability with T–S characteristics of Equatorial Subsurface Water. The coincidence of the T–S properties of the particle maximum with the T–S properties of the subsurface salinity maximum and its association with a minimum in stability indicate a strong relationship between the particle maximum layer and SSW.

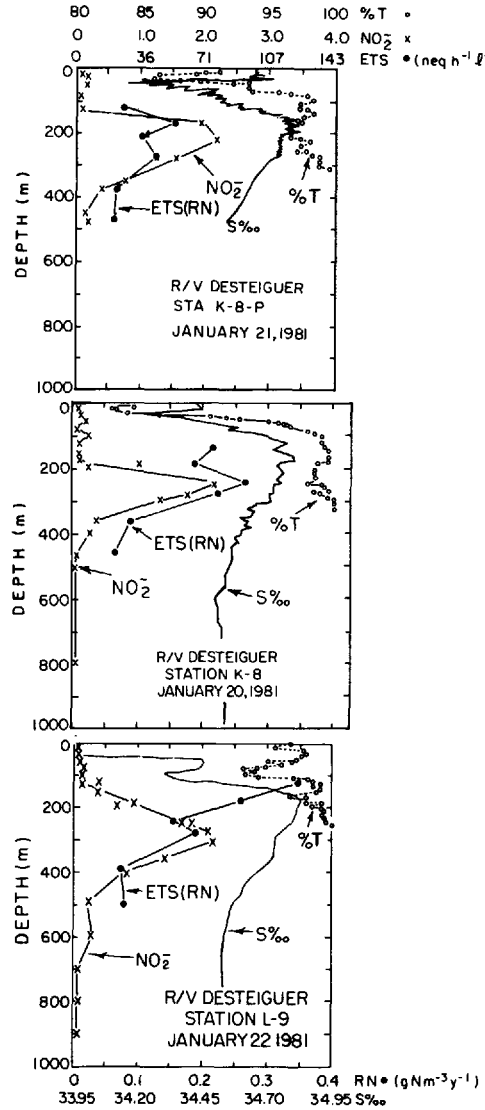

Figure 5. Vertical profiles of temperature (°C), salinity (‰), nitrite concentration (μg-at $NO_2^- - N\ \ell^{-1}$) and ETS activity (neq $\ell^{-1}\ h^{-1}$) at stations where the subsurface maximum in ETS activity was at the same depth as the secondary nitrite maximum. ETS profiles can be interpreted as denitrification rate (RN) in g $Nm^{-3}\ y^{-1}$ on the bottom axis.

The T–S diagrams for stations H-5 and I-6 shown in Figure 7 are for comparison. Although a subsurface salinity maximum was present at both stations, both also show the influence of CCSW. This is seen not only in lower salinities, but also in higher oxygen concentrations and lower nitrite values ($NO_2^- < 0.2$ μg-at ℓ^{-1}) immediately above and within the zone of the subsurface salinity maximum (~50 m) (Figs. 2 and

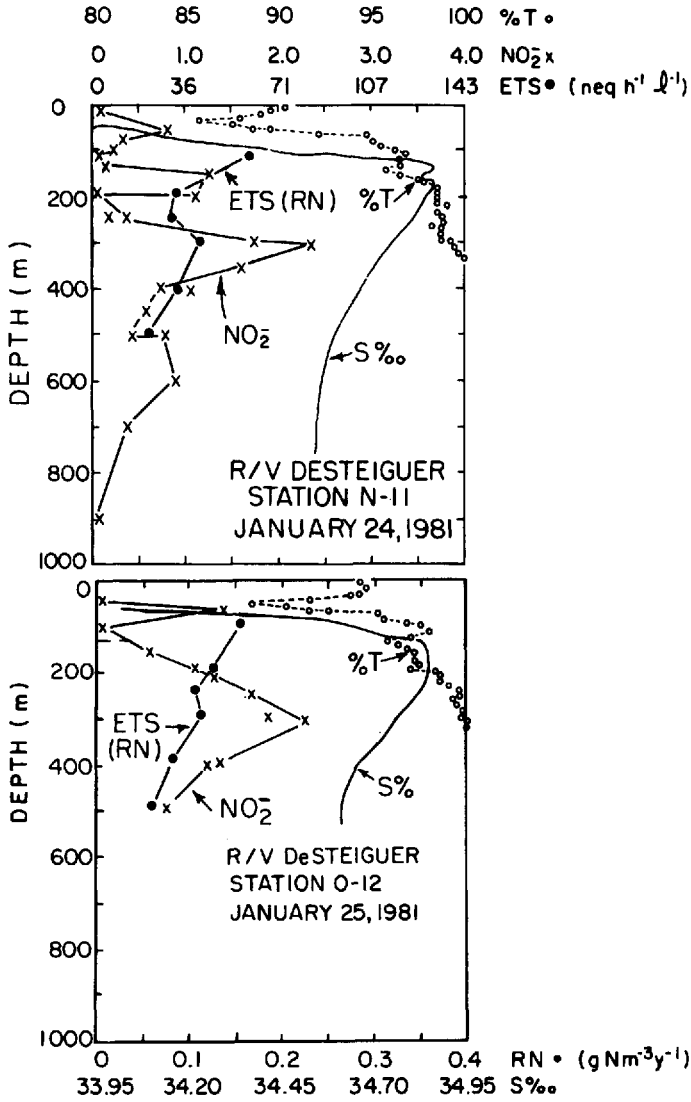

Figure 6. Vertical profiles of temperature (°C), salinity (‰), nitrite concentration (μg-at $NO_2^- - N\ \ell^{-1}$) and ETS activity (neq $\ell^{-1}\ h^{-1}$) at stations where ETS activity did not show a strong peak at the depth of the secondary nitrite maximum. ETS profiles can be interpreted as denitrification rate (RN) in g $Nm^{-3}\ y^{-1}$ on the bottom axis.

4). The mixing processes responsible for these distributions may also destroy the particle maximum layer. A thin particle maximum between 100 and 140 m at J7 was associated with a temperature inversion (Fig. 2) characteristic of frontal structures found in the region of the Gulf of California discharge (LaFond, 1963; Roden, 1964; Griffiths, 1968; Stevenson, 1970). In Figure 7, this particle maximum can be seen at

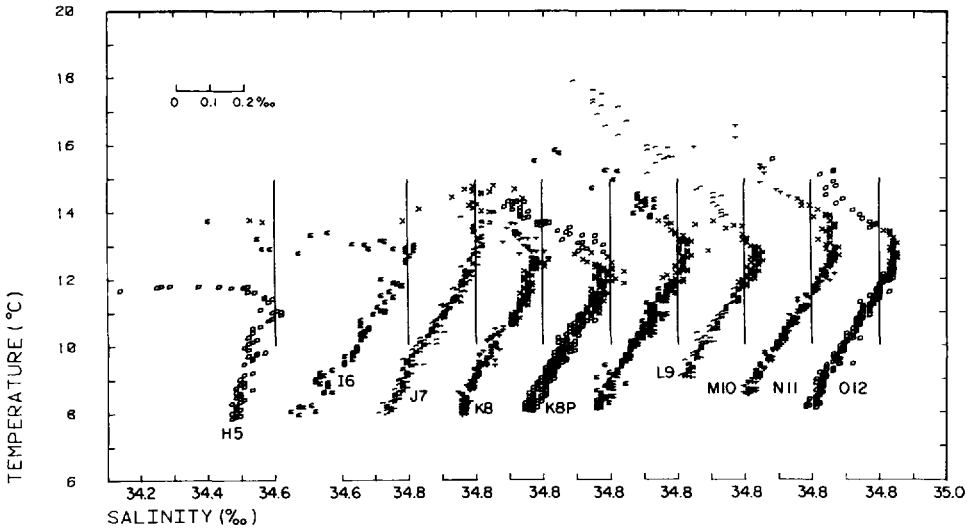

Figure 7. Temperature-salinity diagrams for depths between 100 m and 500 m at stations H5 (far left) to O12 (far right). Each tic mark on the horizontal axis is 0.1‰. The vertical line which intersects each plot marks the 34.8 ‰ values for that plot, with the exception of the plot for H5 where the line marks the 34.6 ‰ values. The symbol "X" denotes values which were within a subsurface particle maximum. Note that these are found at similar T-S values at stations K8 through O12, but are in much warmer water at stations I6 and J7.

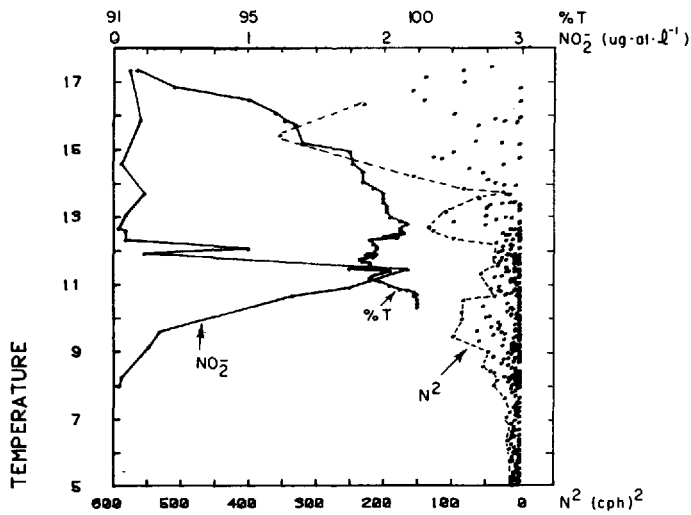

Figure 8. Nitrite concentration (μg-at ℓ^{-1}), transmission (%), and Brunt-Väisälä frequency (N^2, cycles^2 per hour^2) for station K8 plotted as a function of temperature. Depth interval used for N^2 calculations was ~1 m. Dashed line was drawn between maximum values to enclose all data points.

the top of the J7 T–S profile. The salinity is about 34.8‰, but the temperature is too warm to be SSW. Furthermore, there is a distinct maximum in stability at 100 m at J7 which indicates that the particle maximum here is associated with a pycnocline.

d. Distribution of ETS activities. ETS activities showed maxima within the secondary nitrite maximum layer at 3 of the 5 stations where data were collected (Fig. 5), however there was no direct relationship between ETS activity and nitrite concentration such as has been shown for the secondary nitrite maximum off Peru (Codispoti and Packard, 1980). At two of these three stations (K8, K8P), the depth of the particle maximum coincided with the depth of the nitrite maximum and the ETS maximum. At station L9, the % transmission data do not extend to the depth of the nitrite maximum.

ETS activities were higher at all depths at station L9 than at any other station. The value of ~125 neq $h^{-1}\ell^{-1}$ at ~100 m, associated with the thermocline and with a particle maximum at 80–100 m, was the highest value measured during the study period. This particular feature is an interesting result of the circulation of the region that will be discussed later. The ETS activity of ~90 neq $h^{-1}\ell^{-1}$ observed at 150 m at L9 was the second highest value observed during the study period and it occurs at the same depth as the subsurface salinity and particle maximum and within the secondary nitrite maximum (nitrite $\geq$ 0.5 μg-at ℓ^{-1}). It cannot technically be defined as a subsurface ETS maximum because no minimum was observed above it. There was a subsurface ETS maximum at the depth of the nitrite peak (300 m) at this station.

At the two stations (N11, O12) where no subsurface maximum in ETS activity was observed (Fig. 6), no ETS samples were actually taken within the particle maximum layer, so we may have "missed" the ETS maximum. At N11, ETS activity was slightly enhanced in the nitrite peak at 300 m.

In comparison with previously reported ETS activities and ETS-based denitrification rates for the eastern tropical North Pacific Ocean (Packard, 1969; Codispoti, 1973a; Codispoti and Richards, 1976; Devol *et al.,* 1976), these values are higher by a factor of 3–4 (after corrections for all differences in methods). Spatial variability probably accounts for nearly all of the discrepancy. The mean respiration rates reported for this region in the past were taken from the larger general area, while our stations were concentrated in zones where maximum activities were expected. The data from 1972 (Devol, 1975) show that ETS activities at stations where there was a secondary nitrite maximum are about 3 times higher than at stations without this feature. Our results are similar to previous results from individual stations within the secondary nitrite maximum. An increase in ETS activities off Peru between 1969 and 1977 was associated with increased nitrite concentrations, and Codispoti and Packard (1980) have suggested that the total denitrification rate off Peru has increased in recent years. We do not believe that these data are evidence for a similar change here, especially since there has been little or no change in nitrite concentration in this region since 1972.

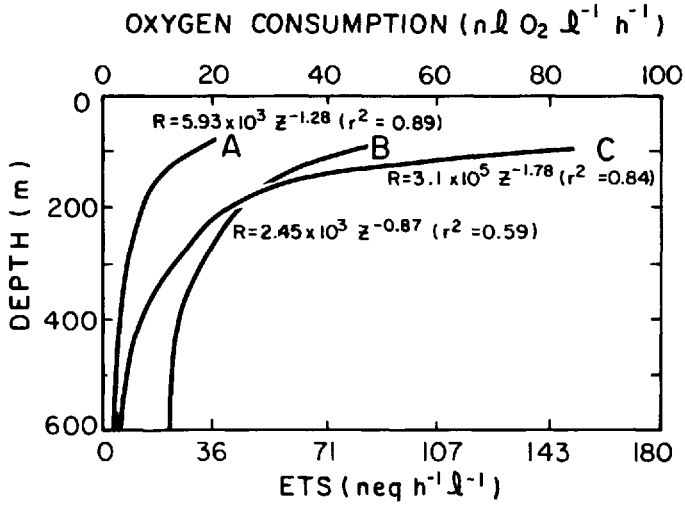

Figure 9. Depth profiles of oxygen consumption rates for three different areas of the ocean: A. mean values for five depths at nine stations in the North Atlantic between 40N, 70W and Bermuda (R/V *Cape Hatteras*, Sept. 1982); B. mean values from this study; C. one station (R/*V Melville* 423) in the Peru upwelling region located at 15.5S, 75.9W (JTII, May 1977). Profiles were generated by fitting the data to a power curve using the equations shown in the figure.

ETS activities measured during this study were converted to oxygen consumption rates to allow comparison with results from other areas (Fig. 9). The depth dependence of respiration rate has been described as an exponential function of the form $R = R_0 e^{-\alpha z}$, where R is the respiration rate at depth Z, R_0 is the respiration rate at the surface, and α is a constant which varies with the properties of the oxidizable organic carbon content of water (Wyrtki, 1962). Previous depth profiles of ETS-derived respiration rates have been found to more closely fit a power function of the form $R = az^{-b}$ (Packard *et al.*, 1983a) and this is the type of equation used to generate the curves in Figure 9. Data from the North Atlantic Ocean were collected aboard the R/V *Cape Hatteras* between Boothbay Harbor, Maine and Bermuda in September 1982 using the same method, filters and sampling intervals used in this study. Respiration rates at intermediate depths (100–500 m) were 3 to 4 times higher off Mexico than in the North Atlantic. The Peru data were taken using the organic extraction method (Packard, 1971; Packard *et al.*, 1971) and Gelman type AE filters. The difference in methods has been accounted for in Figure 9, however, difference in filters was not. Filter comparisons made during the 1981 R/V *De Steiguer* cruise (n=5) and in the laboratory using cultures of marine bacteria (n=34; Packard *et al.*, 1983b) indicate that about twice as much ETS activity is retained by the GF/F filters. This difference could account for the two-fold difference in the data from Mexico and Peru below 200 m.

If elevated respiration rates are a feature of low oxygen concentrations, then the

rates could also be explained by the difference in distribution of oxygen in those two areas. The oxygen-deficient zone ($O_2 < 0.2$ ml ℓ^{-1}) is located between 50 and 500 m at 15S off Peru (Hafferty *et al.*, 1979) and between 100 and 1000 m in the northeastern tropical Pacific Ocean (Codispoti, 1973a). Thus, the high respiration rates above 150 m off Peru are within the oxygen-deficient zone. At 600 m, oxygen concentrations off Peru are increasing and reoxygenation of the water at this depth may explain why the respiration rates begin to converge with values from the North Atlantic.

4. Discussion

Our results add to the body of information suggesting the existence of subsurface maxima in microbial metabolism found in association with the oxygen minimum, nitrite maximum and particle maximum layers. There have been numerous observations of subsurface maxima in microbial biomass in the oceans at the depth of the oxygen minimum (Holm-Hansen and Booth, 1966; Pomeroy and Johannes, 1968; Sorokin, 1972; Devol *et al.*, 1976; Karl *et al.*, 1976; Anderson and Richards, 1977; Karl and Holm-Hansen, 1978; Garfield and Packard, 1979) or at oxic/anoxic interfaces (Karl *et al.*, 1977). A peak in fluorescence associated with the oxygen-nitrite interface in the northeastern Pacific off Mexico may be due to bacterial biomass (Anderson, 1982). Karl and co-workers have evidence (from measurements of RNA synthesis rates) that microbial growth rates are elevated in some of these biomass maxima (Karl, 1979; Fellows *et al.*, 1981).

In all of these cases, the evidence for the subsurface maximum is a small "blip" in a deep profile caused by one or two samples. From data presented in this paper it appears that the layer of maximum activity may be less than 50 m thick, hence, even with a sampling interval of 50 m it is easily missed. Secondly, in some places it may be difficult to separate from the euphotic zone maximum, as at station L9 where no minimum in activity was observed above a high value of ETS activity at 180 m, well within the particle maximum. If each of the above studies were taken separately, the evidence would be far from compelling. However, when all these observations are compiled, the existence of a subsurface microbial biomass peak begins to be plausible. The co-occurrence of peaks in other parameters provides substantiating evidence. The ETS maximum beneath the Peru upwelling is associated with a maximum in particulate protein (Garfield *et al.*, 1979) and with a maximum in particle concentration (Pak *et al.*, 1980; Kullenberg, 1981; Kullenberg and Codispoti, 1982).

One of the most interesting facts which all of these biomass-related maxima have in common is that they all occur at the depth of the oxygen minimum, regardless of whether that oxygen concentration is less than 0.1 ml ℓ^{-1} as in the eastern tropical Pacific or greater than 3 ml ℓ^{-1} as in the North Atlantic. Karl (1982) recently suggested an association between the oxygen minimum, an ATP maximum, and the 27.2 sigma-*t* surface. This relationship does not hold true in the eastern Pacific, where the oxygen minimum is located at sigma-*t* values of between ~26.0 and 26.9 (Figs. 2 and 4;

Hafferty *et al.*, 1979). The oxygen minimum has long been thought to be the result of relatively slow circulation combined with biochemical consumption of oxygen at some rate which is an exponential function of depth. When oxygen concentrations in the source water are low or the surface waters are extraordinarily productive, then oxygen-depleted layers are formed. Increased biomass associated with high growth rates would increase oxygen consumption rates, however, the character of the circulation in an oxygen minimum layer may play an important role in maintaining a localized peak in biomass (see below).

Data from this study provide strong evidence for the existence of a particle maximum at 150–300 m within the subtropical subsurface salinity maximum. The salinity maximum present at I6 and J7 was probably due to the influence of Gulf of California water. The horizontal distribution of SSW is quite extensive as shown by Wyrtki (1967). This water has the same temperature, salinity and density properties as the "Pacific Equatorial 13°C Water" discussed by Tsuchiya (1981), who contends that its place of orgin is the Tasman Sea. The water is transported northward to the equator and then eastward via the Equatorial Undercurrent and the subsurface South Equatorial Countercurrent. At the Galapagos, the water from the undercurrent spreads both north and south. That part which spreads into the North Pacific forms the salinity maximum present throughout the eastern tropical North Pacific. Although the 13°C water is originally high in dissolved oxygen and low in nutrients, lateral mixing and *in situ* nutrient regeneration transform it to a low-oxygen water mass by the time it reaches the eastern boundary. The pattern of bands of high and low oxygen and low and high nutrients apparent near the equator in large-scale maps of the Pacific argue for strong east-west flow patterns and not the cross-meridional flows which might be expected from examining the salinity distributions (Tsuchiya, 1981). The vast horizontal extent of the subsurface salinity maximum is indicative of its relative vertical stability.

The actual source of the particles themselves cannot be established from our data, and no other light scattering data are available for this region. We did not take any data close enough to the shelf edge to determine whether or not that could be the source of the particles, as suggested for other areas (Pak and Zaneveld, 1978; Pak *et al.*, 1980). However, since the salinity maximum is advected into our study area from the southeast, it seems likely that the particles are advected with it, and may even originate as far south as the highly productive surface waters of the Gulf of Tehuantepec or coastal Costa Rica (Love, 1971).

The particles within this maximum must be fairly small, since they do not appear to settle out of SSW over a horizontal distance of roughtly 800 km (K8 to 012). If we assume a horizontal velocity of 5 cm $\cdot$ sec^{-1}, a particle with a sinking rate of ~0.5 m $\cdot$ day^{-1} would sink 100 m in the time required to travel a horizontal distance of 800 km. A change of this magnitude was not observed, so we conclude that particles in this feature had sinking rates of less than 0.5 m $\cdot$ day^{-1} and were smaller than 10 μm in diameter (McCave, 1975).

The shallow particle maximum at 50–100 m at L9 and M10 is associated with a salinity maximum of 34.45‰ and is distinct from the maximum at 200 m. At this level, the water has T-S characteristics similar to those of the surface water at stations K8 and K8P (Fig. 10). Light transmission was low in the surface water at K8 and K8P and productivities were high (0.6–2.0 gC $m^{-2}d^{-1}$; Gaxiola-Castro and Acosta-Puiz, personal communication). Based on the T-S properties and the light scattering properties, one can speculate that the 34.45‰ salinity maximum present at ~100 m at L9 and M10 represents spreading of Subtropical Surface Water to the southwest beneath the less dense Tropical Surface Water.

The 200 m particle maximum is also associated with the secondary nitrite maximum, but it occurs at the level of maximum nitrite concentrations only in the northern part of its range. This is because the core of the nitrite maximum becomes shallower to the north while the depth of the salinity maximum and particle maximum remains constant. A comparison of nitrite concentrations on two different density surfaces for the entire region of the eastern tropical North Pacific (Codispoti, 1973b; Fig. 11) shows that the core of the secondary nitrite maximum is located at a deeper level at 10–15N than at 15–20N. The 26.8 sigma-*t* surface is at about 450 m and the 26.4 surface is at about 200 m depth. While there may be some lateral connection between these two maxima, the one in the south is clearly dissociated from the subsurface salinity maximum, which is at ~100 m off Central America (Wyrtki, 1967). The salinity at the core depth of the southern secondary nitrite maximum is less than 34.6‰.

Nitrite concentrations of less than 0.5 μg-at ℓ^{-1} in the southern part of the salinity maximum indicate that either metabolic rates are relatively low, or that sufficient oxygen is present to support aerobic metabolism. Reliable oxygen concentration data are not available in this region because of the difficulty in measurement at these low levels (<0.25 ml ℓ^{-1}). The nitrite data, however, give some indication of the respiratory progression within the salinity maximum as it travels northwestward along the coast of Central America. The appearance of nitrite on the 26.4 sigma-*t* surface along the northwestward path of the salinity maximum could be the result of total depletion of oxygen by microbial activity and the subsequent switch to denitrification and nitrite reduction.

Formation and composition of the particle maximum layer. One possible mechanism for formation of the 200 m particle maximum which emerges from synthesis of all the above observations is a combination of advection and *in situ* bacterial growth. The T-S properties of this particle maximum and its location within a zone of minimum static stability indicate that it is a feature which is advected into the study region in SSW. The water within the stability minimum should be fairly homogeneous, but there is resistance to mixing across the stability maximum, thereby isolating this depth interval. This explains the extensive horizontal persistence of the feature. The secondary nitrite maximum seems to develop *in situ* from biological activity, as

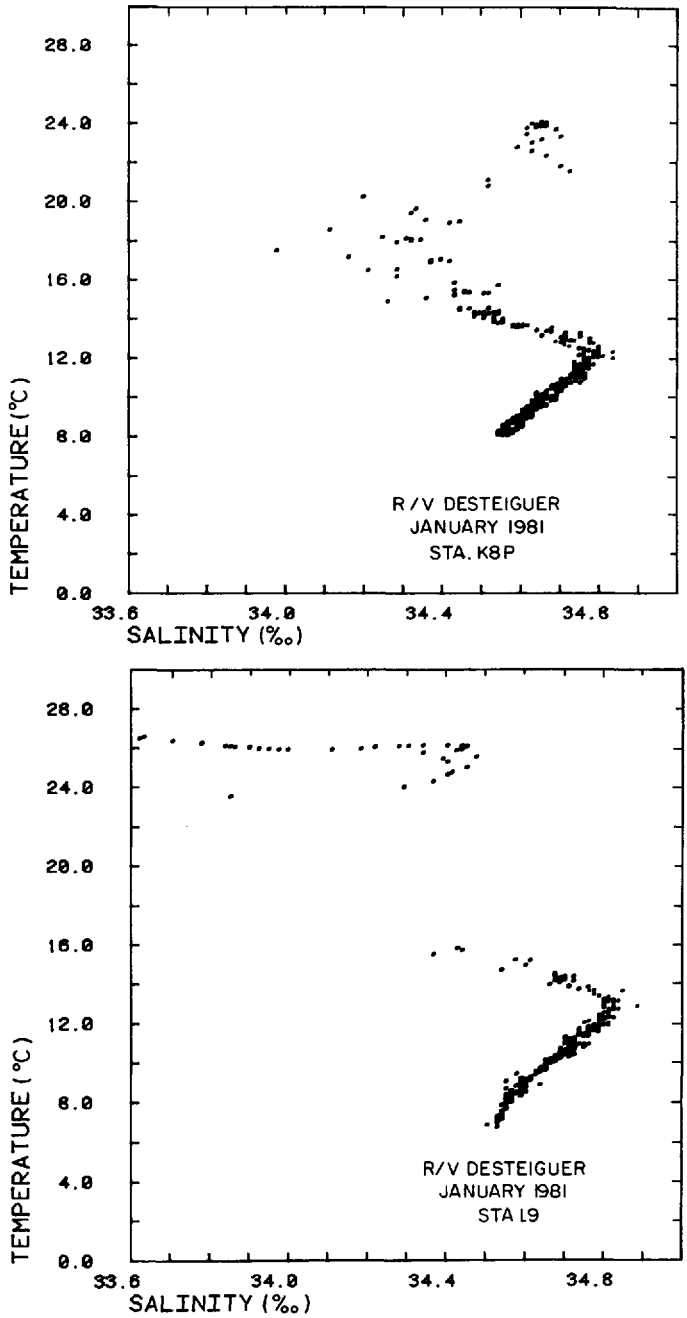

Figure 10. Temperature-salinity plots for stations K8P (top) and L9 (bottom) from the surface to 600 m. Data between 23.7°C and 16.0°C are missing for station L9.

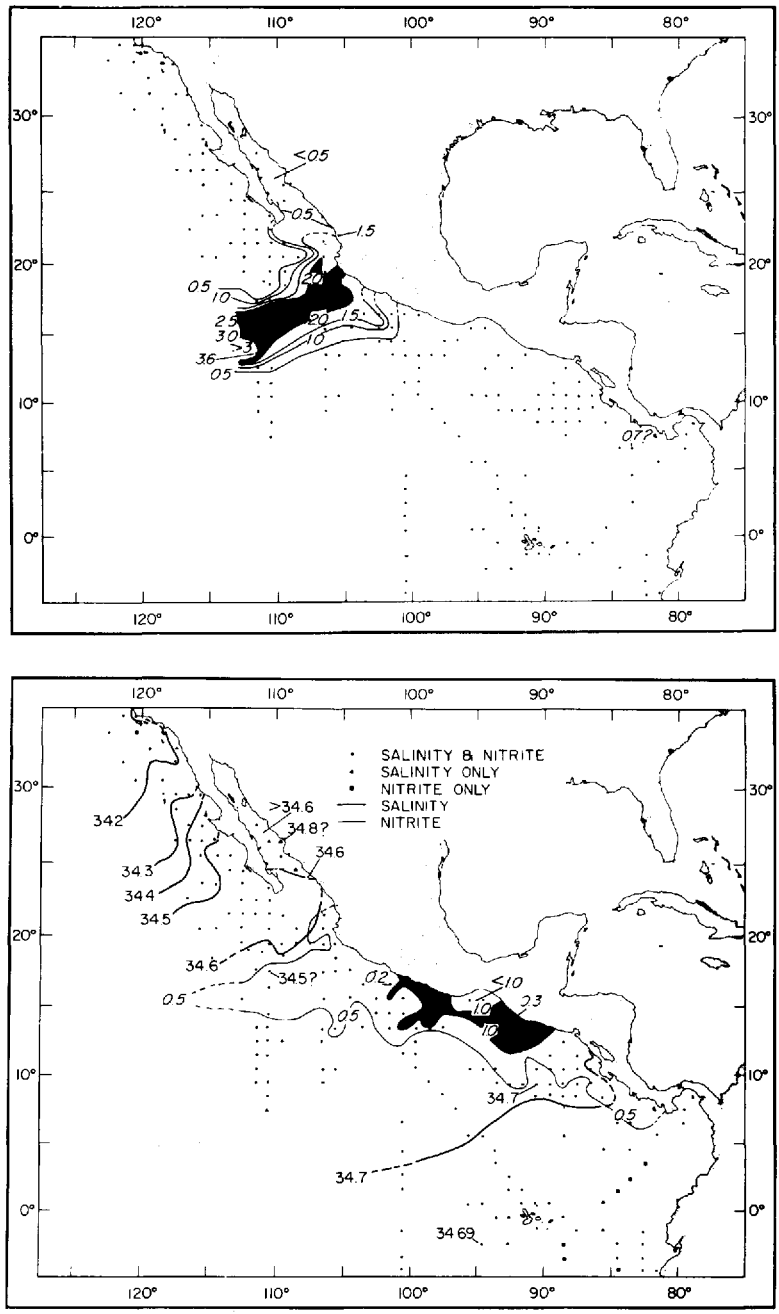

Figure 11. (a) Nitrite concentrations (μg-at ℓ^{-1}) on the 26.4 sigma-t surface. (b) Salinity (‰) and nitrite concentration (μg-at ℓ^{-1}) on the 26.8 sigma-t surface. Both figures redrawn from Codispoti (1973b).

indicated by the appearance of nitrite on the 26.4 sigma-*t* surface along the northwestward path of the salinity maximum (Fig. 11).

The particle maximum undoubtedly consists of some mixture of living, dead organic, and dead inorganic particles. Elevated ETS activities associated with the particle maximum and secondary nitrite maximum represent viable bacterial cells at this depth, although we cannot identify the type of bacteria present on the basis of ETS activity. The low oxygen concentrations combined with high nitrite concentration and nitrate deficit indicate the importance of denitrifying bacteria, however, recent investigations on the ammonium-oxidizing bacteria suggest that they may also be active at oxygen concentrations between 0.1 and 0.5 ml ℓ^{-1} (Goreau *et al.*, 1980). To what extent the particle maximum also represents an increased food supply for bacterial metabolism remains unknown. We have previously suggested that a subsurface maximum in particulate protein observed off Peru could represent a source of organic carbon for heterotrophic bacteria (Garfield *et al.*, 1979).

The bacterial component of this particle maximum layer should not be treated as a totally passive element. Chemotactic responses of bacteria to gradients in organic carbon compounds and electron acceptor concentrations have been well documented and swimming rates of bacterial cells between 10 and 100 $\mu m \cdot sec^{-1}$ have been measured (Rowbury *et al.*, 1983). The oxygen minimum zone is characterized by sharp vertical gradients in chemical parameters, such that a small change in vertical position results in a large change in chemical environment. Since the annual upwelling velocity of SSW in this region is around 20 m yr^{-1} (Wyrtki, 1966), which is equivalent to 0.6 $\mu m \cdot sec^{-1}$, we would expect that motile, chemotactic bacteria present within this water mass would be able to maintain an optimal vertical position. This "active" aspect of the bacteria provides an explanation of why subsurface maxima in microbial biomass and activities may be missed using conventional Niskin bottle depth profiles.

Data from this study suggest a causal relationship between subsurface maxima in particles, nitrite concentrations and ETS activity within oxygen-deficient waters. Definite proof of such a relationship requires further investigation of these areas, including closely-spaced sampling for measurement of all the parameters discussed here plus microscope counts of living vs. dead particles using a stain such as DAPI or acridine orange. Some estimate of bacterial growth rates should also be made to identify levels where cells are actively growing. Such information would greatly increase our understanding of the relative importance of physical, chemical and biological processes in the formation and persistence of subsurface particle maximum layers.

Acknowledgments. This work was funded by ONR Contracts No. N00014-76-C-027 (to TTP) and No. N-00014-81-C-0043 (to LAC) and NSF Contract No. OCE-79-19905. We thank Dr. A. Zirino for the opportunity to participate in the research expedition, N. Garfield for the use of his Brunt-Väisälä frequency program and Dr. G. Kullenberg for numerous helpful discussions. We also thank M. Colby for typing, and J. Rollins for drafting the figures. This is Contribution No. 82032 from the Bigelow Laboratory for Ocean Sciences.

REFERENCES

Anderson, J. J. 1982. The nitrite-oxygen interface at the top of the oxygen minimum zone in the eastern tropical North Pacific. Deep-Sea Res., *29,* 1193–1202.

Anderson, J. J. and F. A. Richards. 1977. Chemical and biochemical observations from the DOMES study area in the equatorial North Pacific. Special Report No. 79, Department of Oceanography, University of Washington, Seattle, WA.

Armstrong, F. A. J., C. R. Stearns and J. D. H. Strickland. 1967. The measurement of upwelling and subsequent biological processes by means of the Technicon Auto-Analyzer and associate equipment. Deep-Sea Res., *14,* 381–389.

Barber, R. T. and A. Huyer. 1979. Nitrite and static stability in the coastal waters off Peru. Geophys. Res. Lett., *6,* 409–412.

Brandhorst, W. 1959. Nitrification and denitrification in the eastern tropical North Pacific. J. du Conseil. Conseil permanent international pour l'exploration de la mer, *25,* 3–20.

Christensen, J. P. and T. G. Owens, A. H. Devol and T. T. Packard. 1980. Respiration and physiological state in marine bacteria. Mar. Biol., *55,* 267–276.

Christensen, J. P. and T. T. Packard. 1979. Respiratory electron transport activities in plankton: Comparison of methods. Limnol. Oceanogr., *24,* 576–583.

Cline, J. D. and F. A. Richards. 1972. Oxygen deficient conditions and nitrate reduction in the eastern tropical North Pacific Ocean. Limnol. Oceanogr., *17,* 885–900.

Codispoti, L. A. 1973a. Denitrification in the eastern tropical North Pacific Ocean. Ph.D. thesis, University of Washington, Seattle, WA, 118 pp.

—— 1973b. Some physical and chemical properties of the eastern tropical North Pacific with emphasis on the oxygen minimum layer. University of Washington, Department of Oceanography Technical Report 289, 40 pp.

Codispoti, L. A. and T. T. Packard. 1980. Denitrification rates in the eastern tropical South Pacific. J. Mar. Res., *38,* 453–477.

Codispoti, L. A. and F. A. Richards. 1976. An analysis of the horizontal regime of denitrification in the eastern tropical North Pacific. Limnol. Oceanogr., *21,* 379–388.

Devol, A. H. 1975. Biological oxidations in oxic and anoxic marine environments: Rates and processes. Ph.D. thesis, University of Washington, Seattle, WA, 208 pp.

Devol, A. H., T. T. Packard and O. Holm-Hansen. 1976. Respiratory electron transport activity and adenosine triphosphate in the oxygen minimum of the eastern tropical North Pacific. Deep-Sea Res., *23,* 963–973.

Fellows, D. A., D. M. Karl and G. A. Knauer. 1981. Large particle fluxes and the vertical transport of living carbon in the upper 1500 m of the northeast Pacific Ocean. Deep-Sea Res., *28,* 921–936.

Friederich, G. E. and T. E. Whitledge. 1972. AutoAnalyzer procedure for nutrients, *in* Phytoplankton Growth Dynamics, S. P. Pavlou, ed., University of Washington, Department of Oceanography, Special Publication 52, unpublished document.

Garfield, P. C. 1982. Physical, chemical and biological data from Varifront II, R/V *DeSteiguer,* Jan. 1981. Bigelow Laboratory Technical Report No. 29.

Garfield, P. C. and T. T. Packard. 1979. Biological data from JOINT II R/V *Melville,* Leg IV. May 1977. Coastal Upwelling Ecosystems Analysis Technical Report No. 53, 186 pp.

Garfield, P. C., T. T. Packard and L. A. Codispoti. 1979. Particulate protein in the Peru upwelling system. Deep-Sea Res., *26,* 623–639.

Goering, J. J. 1968. Denitrification in the oxygen minimum layer of the eastern tropical Pacific Ocean. Deep-Sea Res., *15,* 151–164.

Goreau, T. J., W. A. Kaplan, S. C. Wofsy, M. B. McElroy, F. W. Valois and S. W. Watson. 1980. Production of NO_2^- and N_2O by nitrifying bacteria at reduced concentrations of oxygen. Appl. Environ. Microbiol., *40,* 526–532.

Griffiths, R. C. 1965. A study of ocean fronts off Cape San Lucas, Lower California. U.S. Fish. Wildl. Serv., Spec. Sci. Rept. Fish., 499, iv + 54 pp.

—— 1968. Physical, chemical, and biological oceanography of the entrance to the Gulf of California, Spring of 1960. U.S. Fish Wildl. Serv. Spec. Sci. Rept., 573, 47 pp.

Hafferty, A. J., D. Lowman and L. A. Codispoti. 1979. JOINT-II, *Melville* and *Iselin* bottle data sections, March–May 1977. Coastal Upwelling Ecosystems Analysis Technical Report 38, 129 pp.

Holm-Hansen, O. and C. R. Booth. 1966. The measurement of adenosine triphosphate in the ocean and its ecological significance. Limnol. Oceanogr., *11,* 510–519.

Karl, D. M. 1979. Measurement of microbial activity and growth in the ocean by rates of stable ribonucleic acid synthesis. Appl. Environ. Microbiol., *38,* 850–860.

—— 1982. Microbial transformations of organic matter at oceanic interfaces: A review and prospectus. EOS, *63,* 138–140.

Karl, D. M. and O. Holm-Hansen. 1978. Methodology and measurement of adenylate energy charge ratios in environmental samples. Mar. Biol., *48,* 185–197.

Karl, D. M., P. A. La Rock, J. W. Morse and W. Sturges. 1976. Adenosine triphosphate in the North Atlantic Ocean and its relationship to the oxygen minimum. Deep-Sea Res., *23,* 81–88.

Karl, D. M., P. A. La Rock and D. J. Shultz. 1977. Adenosine triphosphate and organic carbon in the Cariaco Trench. Deep-Sea Res., *24,* 105–113.

Kenner, R. A. and S. I. Ahmed. 1975. Measurement of electron transport activities in marine phytoplankton. Mar. Biol., *33,* 119–128.

Kullenberg, G. 1981. A comparison of distributions of suspended matter in the Peru and Northwest Africa upwelling areas, *in* Coastal Upwelling, F. A. Richards, ed., AGU, Washington, D.C., 282–290.

Kullenberg, G. and L. A. Codispoti. 1982. On the distribution of suspended matter in and off the Peru upwelling area, unpublished manuscript.

LaFond, E. C. 1963. Detailed temperature structure of the sea off Baja California. Limnol. Oceanogr., *8,* 417–425.

Love, C. M. editor. 1971. EASTROPAC Atlas, vol. 2, United States Department of Commerce, Washington, D.C., Circular 330, vii pp., 296 figures.

McCave, I. N. 1975. Vertical flux of particles in the ocean. Deep-Sea Res., *22,* 491–502.

Murphy, J. and J. P. Riley. 1962. A modified single solution method for the determination of phosphate in natural waters. Anal. Chim. Acta, *27,* 31–36.

Packard, T. T. 1969. The estimation of the oxygen utilization rate in seawater from the activity of the respiratory electron transport system in plankton. Ph.D. thesis, University of Washington, Department of Oceanography, Seattle, WA, 115 pp.

—— 1971. The measurement of respiratory electron transport activity in marine phytoplankton. J. Mar. Res., *29,* 235–244.

Packard, T. T., P. C. Garfield and L. A. Codispoti. 1983a. Oxygen consumption and denitrification below the Peruvian Upwelling, *in* Coastal Upwelling, Pt. A, E. Suess and J. Thiede, eds., Plenum Press, 147–173.

Packard, T. T., P. C. Garfield and R. Martinez. 1983b. Respiration and respiratory enzyme activity in aerobic and anaerobic cultures of the marine denitrifying bacterium, *Pseudomonas perfectomarinus.* Deep-Sea Res., *30,* 227–243.

Packard, T. T., M. L. Healy and F. A. Richards. 1971. Vertical distribution of the activity of the respiratory electron transport system in marine plankton. Limnol. Oceanogr., *16,* 60–70.

Packard, T. T. and P. J. LeB. Williams. 1981. Rates of respiratory oxygen consumption and electron transport in surface seawater from the Northwest Atlantic. Oceanol. Acta, *4,* 351–358.

Pak, H., L. A. Codispoti and J. R. V. Zaneveld. 1980. On the intermediate particle maxima associated with oxygen-poor water off western South America. Deep-Sea Res., 27A, 783–797.

Pak, H. and J. R. V. Zaneveld. 1978. Intermediate nepheloid layers observed on the continental margin off Oregon. Society of Photo-optical Instrument engineers, *160,* 9–17.

Pomeroy, L. R. and R. E. Johannes. 1968. Occurrence and respiration of ultraplankton in the upper 500 meters of the ocean. Deep-Sea Res., *15,* 381–391.

Roden, G. I. 1964. Shallow temperature inversions in the Pacific Ocean. J. Geophys. Res., *69,* 2899–2914.

—— 1971. Aspects of the transition zone in the northeastern Pacific. J. Geophys. Res., *76,* 3462–3475.

Roden, G. I. and G. W. Groves. 1959. Recent oceanographic investigations in the Gulf of California. J. Mar. Res., *18,* 10–35.

Rowbury, R. J., J. P. Armitage and C. King. 1983. Movement, taxes and cellular interactions in the response of microorganisms to the natural environment, *in* Microbes in their Natural Environments, J. H. Slater, R. Whittenbury and J. W. T. Wimpenny, eds., Symposium 34. Soc. for Gen. Microbiol. Ltd., Cambridge University Press.

Slawyk, G. and J. J. MacIsaac. 1972. Comparison of two automated ammonium methods in a region of coastal upwelling. Deep-Sea Res., *19,* 521–524.

Sorokin, Y. I. 1972. Microbial activity as a biogeochemical factor in the ocean, *in* The Changing Chemistry of the Oceans, D. Drysden and D. Jagner, eds., Wiley-Interscience, Almquist, Stockholm, 189–204.

Stevenson, M. R. 1970. On the physical and biological oceanography near the entrance of the Gulf of California, October 1966–August 1967. Inter-American Tropical Tuna Commission Bulletin, *14,* No. 3, 389–504.

Thomas, W. H. 1966. On denitrification in the northeastern tropical Pacific Ocean. Deep-Sea Res., *13,* 1109–1114.

Tsuchiya, M. 1981. The origin of the Pacific Equatorial 13°C water. J. Phys. Oceanogr., *11,* 794–812.

Wyrtki, K. 1962. The oxygen minima in relation to oceanic circulation. Deep-Sea Res., *9,* 11–23.

—— 1966. Oceanography of the eastern equatorial Pacific Ocean. Oceanogr. Mar. Biol. Ann. Rev., *4,* 33–68.

—— 1967. Circulation and water masses in the eastern equatorial Pacific Ocean. Int. J. Oceanol. Limnol., *1,* 117–147.

Received: *30 November, 1982;* revised: *23 June, 1983.*